Regression-based Main Bearing Load Estimation

Amin Loriemi[1], Georg Jacobs[1], Vitali Züch[1], Timm Jakobs[1], Dennis Bosse[1]

[1]Chair for Wind Power Drives, RWTH Aachen, Aachen, 52074, Germany

Correspondence to: Amin Loriemi (amin.loriemi@cwd.rwth-aachen.de)

Abstract. The premature failure of wind turbines due to unknown loads leads to a reduction in competitiveness compared to other energy sources. Especially the failure of main bearings results in high costs and downtimes, as for an exchange of this component the rotor needs to be demounted. Load monitoring systems can make a significant contribution to understand and prevent such failures. However, most load monitoring systems do not take into account the main bearing loads in particular as there is no commercially applicable measuring system for this purpose. This work shows how main bearing loads can be estimated using virtual sensors. For this purpose, several regression models are trained with test bench data considering strain and displacement signals. It is investigated with which combination of signal type and regression model the highest accuracy is achieved. The results show that for either using strain or displacement signals an appropriate accuracy can be achieved. In particular, it is shown that a linear regression with interactions already achieves good accuracy and that further increases in regression model complexity do not add significant value.

1 Introduction

Over the last decades the size of wind turbines continuously increased (Enevoldsen and Xydis, 2019). The rising rotor diameter results in higher torque but also overproportional higher non-torque loads, which are acting on main bearings (MB) of wind turbines. But even designed after state-of-the-art guidelines premature failures of these bearings occur. In this context, studies which consider main bearing failures of entire fleets report for a target lifetime of 20 year, failure rates up to 30 % (Hart et al., 2019) or a premature failure before 6 years of operation (Yucesan and Viana, 2019). Since main bearing design and rolling element selection is made based on fatigue life and static load ratings only, the reported premature failures could also be explained by other damage and wear mechanisms like micro-pitting, spalling, smearing or fretting (Hart et al., 2020). Nevertheless, all these damage mechanisms are load-driven and therefore a better understanding of the underlying damage patterns requires a detailed knowledge of the main bearing loads. A direct measurement of main bearing loads is not possible as there are no force transducers available for this load range. So a load estimation based on measurable variables is necessary. In this work, the main bearing load estimation based on strain and displacement signals is evaluated with regard to its achievable accuracy. For this purpose, a low wind speed turbine was examined on a full-size test bench. Strain and displacement signals under dynamic load time series were recorded. On the basis of the obtained data, fourteen regression

models are trained and their accuracy is evaluated. It is investigated which kind of combination regarding signal type and
30 regression model achieves best accuracy to derive recommendations for an appropriate load monitoring system.

2 Background

The main bearing historically has not been focused in reports of failing wind turbine components. It is usually not accurately documented which operational loads have led to main bearing failures and what have been the underlying damage mechanisms (Hart et al., 2020). Additionally, main bearing loads per se are not recorded in traditional data acquisition from wind turbines.
35 A classic supervisory control and data acquisition (SCADA) system of a wind turbines, mainly logs its performance parameters like the rotational speed of the low or high speed shaft, wind speed at hub height, pitch angles, temperatures or generated electric power. Thereby mean, maximum and minimum values are recorded covering a time span of up to ten minutes. Various approaches attempt to reproduce the acting loads from these data. Pagitsch et al (Pagitsch et al., 2020) use simplified rotor, transmission and generator models to enable a main bearing load estimation based on SCADA data. Due to the underlying
40 data properties, however, the approach chosen here only allows the calculation of statistical load distributions. A time-resolved estimation of main bearing loads and the representation of transient events is not enabled by this approach. Other methods use artificial neural networks (ANN) to estimate single load components such as thrust acting on a wind turbine with a time resolution of one second (Noppe et al., 2018). But this gives only partial information on the complete main bearing loading what complicates a later detailed understanding of harmful load situations. It can be concluded from this that a load monitoring
45 on the basis of classic SCADA data is hardly possible and additional sensors are necessary to fulfil this task.

Various sensor technologies are available to measure main bearing related loads with additional sensors. Hereby, the measurement of strains has been a method widely used especially in prototype validation and certification of wind turbines. Regarding main bearing loads, strain gauges are typically applied to the main shaft after the first main bearing. Here, especially bending strains, torsional strains and eventually strains due to axial main shaft loading can be measured. Without calibration,
50 assuming the main shaft as a beam, a linear relationship between strain and cross-sectional loads can be derived using beam theory (Lekou and Mouzakis, 2009). On basis of these cross-sectional loads corresponding main bearing loads could be calculated. Unfortunately, these methods are subject to uncertainties due to a corresponding variance of the young modulus and strain gauge positioning (Guy, 2015; Kock et al., 2018). To overcome these problems a load-based calibration can be performed (Lekou and Mouzakis, 2009). But this is only possible for a load range, which is rather limited with respect to the
55 expected load range in operation (Bezziccheri et al., 2017). Additionally, classic strain gauges suffer from signal drift (Berg et al., 2014; Verbruggen et al., 2012) and have a limited lifetime of typically a few years (Verbruggen et al., 2012), which makes this technology inappropriate for a long-term application with a 20 year target life time. Finally, precise and durable force sensors, which are also based on strain measurement, are not available on the market in the dimension required for this application and their concepts are designed for the measurement of single load components. Even though there are concepts
60 for multicomponent transducers for measuring the rotor loads of multimegawatt wind turbines (Gnauert et al., 2020), their

technical realization has not yet been taken place and it remains questionable whether their use will be economical in series production or only suitable for validation tasks.

Alternatively, local displacement signals near the main bearings could be used to estimate main bearing loads. Compared to strain gauges, displacement sensors are robust, durable and easy to install, which makes them particularly interesting for this application. Concepts to measure loads using displacement signals do exist in the context of rotor load estimation for wind turbine control (Pierce and Lemieux, 2007; Pierce et al., 2006). Unlike strain signals, displacement signals do not necessarily have a linear relationship to corresponding loads. In the application of main bearing load estimation, progressive bearing stiffness behavior and discontinuities due to bearing clearance make it particularly difficult to convert displacements directly into loads. Simulation-based studies have shown that a displacement-based main bearing load estimation using artificial neural networks promises a good accuracy, while the use of linear regression models does have the advantage of a more robust behavior due to main bearing clearance uncertainties (Loriemi et al., 2022).

3 Methods

This section describes the test setup used to obtain data for main bearing load estimation. A description regarding the differentiation between training and testing data is given. Finally, the regression models used for estimation are explained.

3.1 Experimental Setup

This study is based on measurements obtained at the full-size test bench of the Center for Wind Power Drives (CWD) (Reisch et al., 2017). The test bench enables the testing of wind turbine nacelles by applying rotor loads in alle six degrees of freedom. This has been done in the context of prototype validation of the low wind speed turbine maxcap141 (Becker, 2019). Figure 1 shows the test setup.
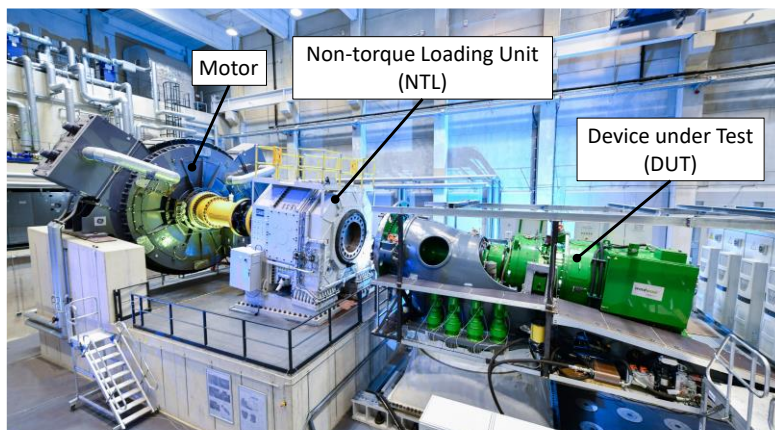
Figure 1. Test Setup for prototype validation of maxcap141 at Centre for Wind Power Drives
[credits: MWIDE NRW/Andreas Buck/maxcap-windwise GmbH]

In this test setup, input torque is generated by the test bench motor. Non-torque loads like bending moments, transversal forces and thrust are applied by the non-torque loading unit (NTL) and transmitted to the rotor flange of the device under test (DUT).

85   The DUT is the nacelle of a maxcap141, a 2.3 MW low wind speed turbine (rotor diameter: 141 m; nominal wind speed: 9 m/s) that has been developed in the context of the project 'MaxCap' (Becker, 2019). The rotor suspension system is designed as a four-point suspension, as it is shown in Figure 2. The main bearing arrangement consists of a cylindrical roller bearing as a floating bearing (FB) and a double row tapered roller bearing in x-arrangement as a locating bearing (LB) are used as main bearings. The gearbox is connected to the machine carrier by a hydraulic suspension as torque supports (TS). This type of

90   torque supports is characterized by a high torsional stiffness, whereas a translational movement of the gearbox in relation to the machine carrier is only met with a low resistance (Helsen et al., 2014). Thereby, the rotor input torque is supported only by this component, leaving non-torque loads being supported mostly by the main bearings. The generator is directly mounted to the gearbox and supported by an elastomeric generator support (GS). Considering stiffness behavior of the TS and GS, a direct calculation of the main bearing loads from loads applied by the NTL is not possible, as the mechanical system is

95   overdetermined. Neglecting reactions forces of the TS and GS may lead to an overestimation of the main bearing loads.
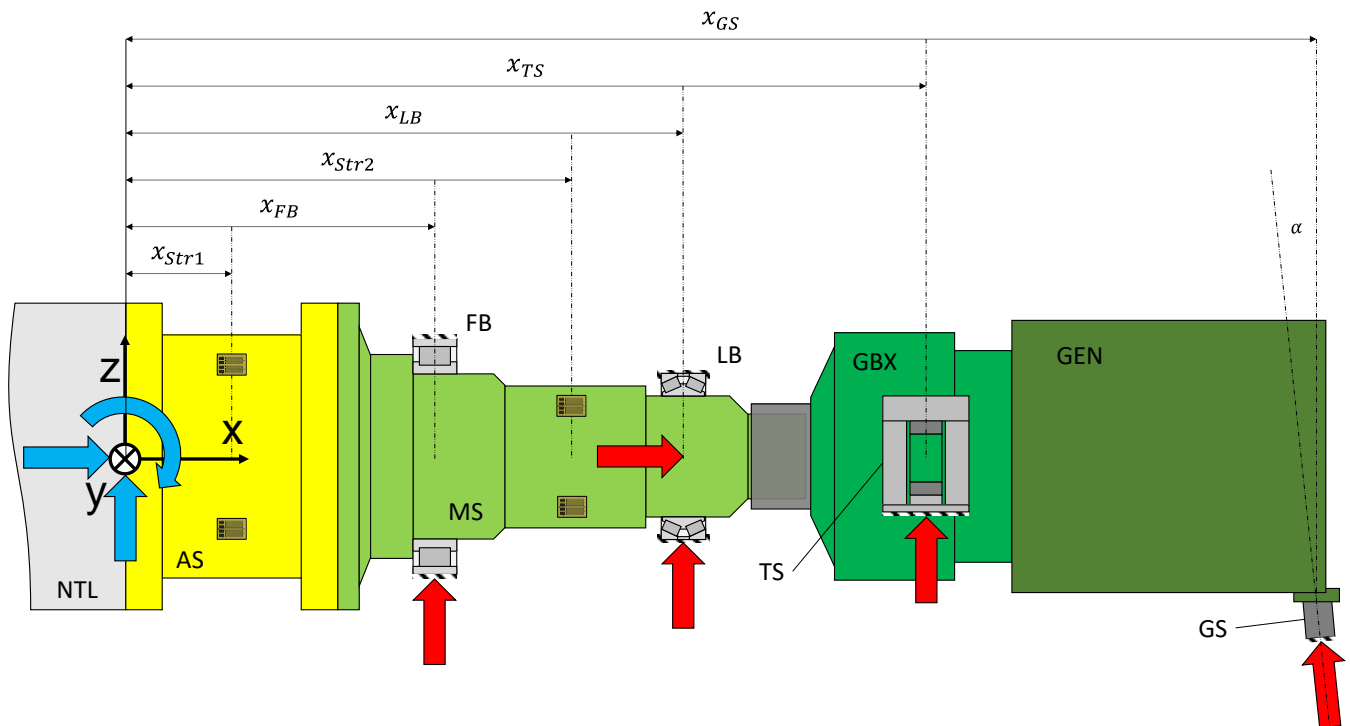
Figure 2. Principle sketch of drivetrain assembly

For that reason in this analysis these reaction forces are considered and main bearing loads are calculated as follows:

$$F_{y,FB} = \frac{x_{LB}(F_{y,NTL}+F_{y,TS}+F_{y,GS})-x_{GS}\cdot F_{y,GS}-x_{TS}\cdot F_{y,TS}-M_{z,NTL}}{x_{FB}-x_{LB}} \tag{1}$$

$$F_{z,FB} = \frac{x_{LB}(F_{z,NTL}+F_{z,TS}+F_{z,GS})-x_{GS}\cdot F_{y,GS}-x_{TS}\cdot F_{y,TS}+M_{y,NTL}}{x_{FB}-x_{LB}} \tag{2}$$

$$F_{x,LB} = -F_{x,TS}-F_{x,GS}-F_{x,NTL} \tag{3}$$

$$F_{y,LB} = \frac{-x_{LB}(F_{y,NTL}+F_{y,TS}+F_{y,GS})+x_{GS}\cdot F_{y,GS}+x_{TS}\cdot F_{y,TS}+M_{z,NTL}}{x_{FB}-x_{LB}} \tag{4}$$

$$F_{z,LB} = \frac{x_{LB}(F_{z,NTL}+F_{z,TS}+F_{z,GS})-x_{GS}\cdot F_{z,GS}-x_{TS}\cdot F_{z,TS}-M_{y,NTL}}{x_{FB}-x_{LB}} \tag{5}$$

In the test setup, non-torque loads applied by the NTL ($F_{x,NTL}$, $F_{y,NTL}$, $F_{z,NTL}$, $M_{y,NTL}$, $M_{z,NTL}$) are calculated from measurements of the NTL's hydraulic actuators. According to equations 1-5 the reaction forces of the torque supports ($F_{x,TS}$, $F_{y,TS}$, $F_{z,TS}$) and generator support ($F_{x,GS}$, $F_{y,GS}$, $F_{z,GS}$) has to be known as well to calculate main bearing loads. This is done by displacement measurement at these components using Linear Variable Differential Transformers (LVDT). In the preparation of the tests, the TS and GS were measured on component test benches and three-dimensional stiffness curves were recorded. This allows to calculate the reaction forces of these components.

As described before, strain and displacement signals are used for main bearing load estimation. For this purpose, full strain-gauge bridges were applied on the main shaft (MS) and also on the adapter shaft (AS), which is connecting the MS to the NTL in the test setup. At each position (x_{Str1} and x_{Str2} in Figure 2) there are two full bridges offset to each other by 90° using strain gauges, which enables the measurement of pure bending strains. Before testing all full bridges have been shunt calibrated. No full bridge for measuring pure tensile strains were available in the setup and therefore a measurement of axial loads using strain signals was not possible. However, it must be noted that the DUT is a low wind speed turbine, which is characterized by a rather large rotor. The measurement of pure thrust-induced strains would therefore only have been possible with a significantly worse signal-to-noise-ratio.

Additionally to the strain gauges, sixteen eddy current sensors have been applied to measure local displacements at the main bearing locations as shown in Figure 3. To evaluate more general variables for load estimation, these single axial and radial displacement signals are post-processed and an overall translational or rotational displacement of the main shaft is calculated as follows (according to Figure 4):

$$\begin{pmatrix} u_{rad1} \\ u_{rad2} \\ u_{rad3} \\ u_{rad4} \\ u_{ax1} \\ u_{ax2} \\ u_{ax3} \\ u_{ax4} \end{pmatrix} = \begin{pmatrix} 0 & -\cos\alpha & -\sin\alpha & 0 & 0 \\ 0 & -\cos\beta & -\sin\beta & 0 & 0 \\ 0 & -\cos\gamma & -\sin\gamma & 0 & 0 \\ 0 & -\cos\delta & -\sin\delta & 0 & 0 \\ -1 & 0 & 0 & -r\sin\alpha & -r\cos\alpha \\ -1 & 0 & 0 & -r\sin\beta & -r\cos\beta \\ -1 & 0 & 0 & -r\sin\gamma & -r\cos\gamma \\ -1 & 0 & 0 & -r\sin\delta & -r\cos\delta \end{pmatrix} \cdot \begin{pmatrix} u_x \\ u_y \\ u_z \\ \varphi_y \\ \varphi_z \end{pmatrix} \tag{6}$$
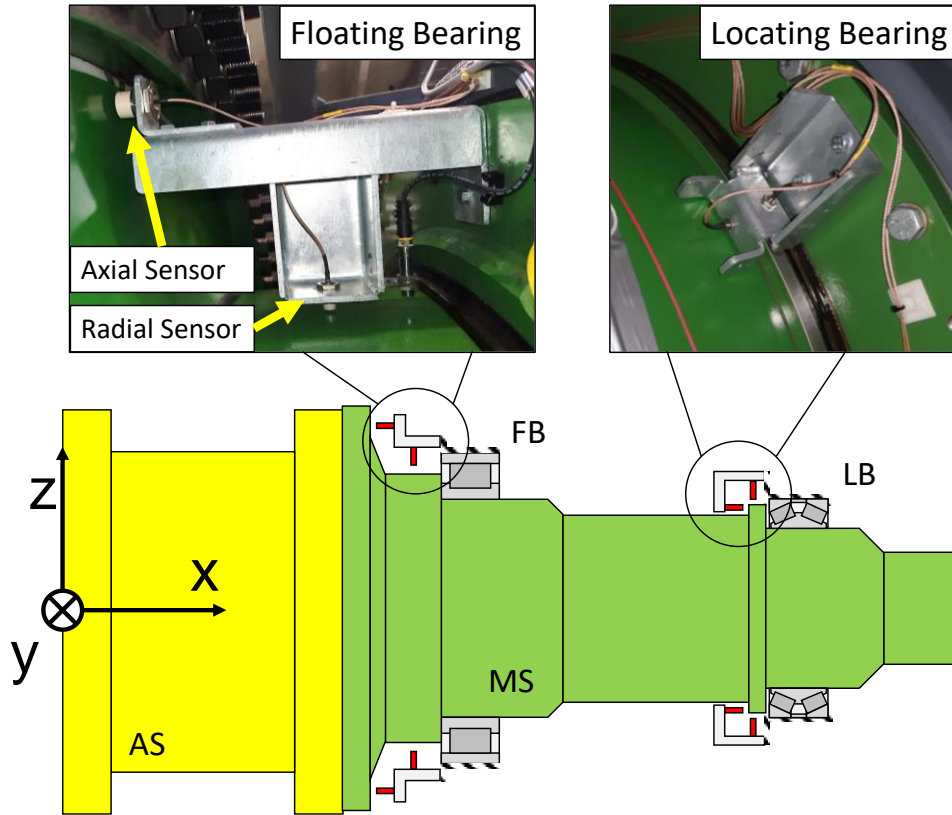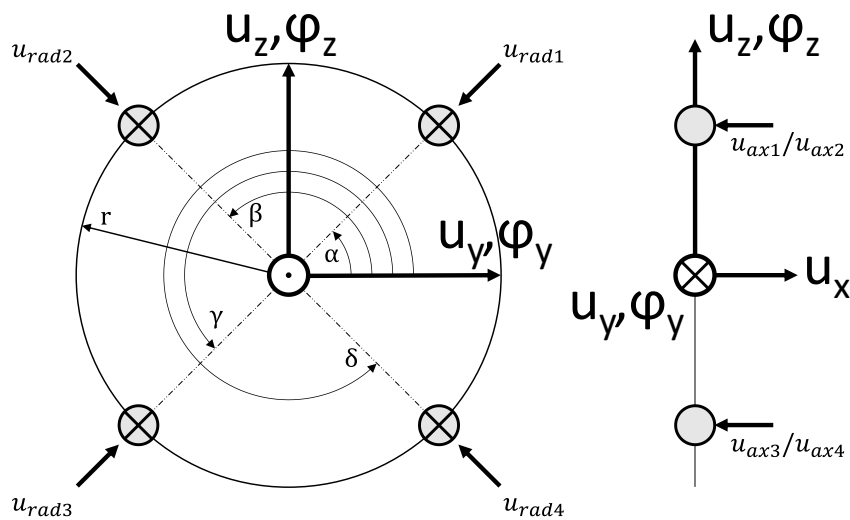
Figure 3. Displacement Sensors

Figure 4. Principle sketch of displacement signal post-processing

130

Equation (6) clarifies that less sensors (at least five) could be used to evaluate the five target variables at each bearing location. Nevertheless, in this study all available sensors are used to derive a more averaged measurement.

3.2 Test Plan

135 Main bearings are exposed to a complex, highly dynamic loading situation. In order to adequately evaluate the performance of the regression models, realistic loads should be considered. Therefore, load time series obtained by multibody simulation (MBS) in accordance to IEC 61400 for turbulent wind fields are applied to the DUT. Thereby not only wind speed but also wind class is varied. For every wind speed and wind class combination six ten-minute time series are obtained. Specifications can be taken from Table 1.

Table 1. Specification of measurement campaign

Intended Use	Wind Speed (Incrementation)	Wind Class (Turbulence Intensity)
Training Data	3 m/s to 12 m/s (1 m/s)	IIa (High)
Testing Data	3 m/s to 12 m/s (1 m/s)	IIb (Moderate)
Training Data	3 m/s to 12 m/s (1 m/s)	IIc (Low)

140

As can be seen in Table 1, a separation between training and testing data is made depending on the wind class. Since data-driven models are used for main bearing load estimation, their performance depends significantly on the training data and to what extent they cover the intended application. In order to provide good preconditions, low and high turbulence intensities are selected for the time series of the training data. Thereby training data conceptionally frames the loads within testing data

145 of moderate turbulence intensities.

3.3 Strain-based load estimation

A pure strain-based load estimation is performed using only strain signals measured by the installed strain gauges. In a first approach a physically motivated approach is chosen for main bearing load estimation. Neglecting the small stiffnesses of the TS and GS, a simplified system of equations can be developed from beam theory, describing the relationship between bending

150 strains and main bearing radial loads analytically as follows:

$$F_{y,FB} = \frac{E_{Str1} \cdot S_{Str1} \cdot (x_{LB} - x_{Str2})}{(x_{LB} - x_{Str1}) \cdot (x_{LB} - x_{Str2})} \cdot \varepsilon_{zStr1} - \frac{E_{Str2} \cdot S_{Str2} \cdot (x_{LB} - x_{Str1})}{(x_{LB} - x_{Str1}) \cdot (x_{LB} - x_{Str2})} \cdot \varepsilon_{zStr2} \tag{6}$$

$$F_{z,FB} = \frac{E_{Str1} \cdot S_{Str1} (x_{LB} - x_{Str2})}{(x_{LB} - x_{Str1}) \cdot (x_{LB} - x_{Str2})} \cdot \varepsilon_{yStr1} - \frac{E_{Str2} \cdot S_{Str2} \cdot (x_{LB} - x_{Str1})}{(x_{LB} - x_{Str1}) \cdot (x_{LB} - x_{Str2})} \cdot \varepsilon_{yStr2} \tag{7}$$

$$F_{y,LB} = \frac{E_{Str2} \cdot S_{Str2}}{x_{LB} - x_{Str2}} \cdot \varepsilon_{zStr2} \tag{8}$$

155 $$F_{z,LB} = -\frac{E_{Str2} \cdot S_{Str2} \cdot}{x_{LB} - x_{Str2}} \cdot \varepsilon_{yStr2} \tag{9}$$

$\varepsilon_{y/z\ Str1/2}$:   Bending strain in y/z-direction at location Str1/Str2

$E_{Str1/2}$:   Young modulus at location Str1/Str2

$S_{Str1/2}$:   Section modulus at location Str1/Str2

160   As described before, this physics-based approach is subject to uncertainties, but serves as a reference in this work. When strain gauges are used in practice, load-based calibration is performed whenever possible. Accordingly, a second model is developed using a linear regression as follows:

$$F_{y,FB} = a_1 \cdot \varepsilon_{zStr1} + a_2 \cdot \varepsilon_{zStr2} \tag{10}$$

165    $$F_{z,FB} = a_3 \cdot \varepsilon_{yStr1} + a_4 \cdot \varepsilon_{yStr2} \tag{11}$$

$$F_{y,LB} = a_5 \cdot \varepsilon_{zStr2} \tag{12}$$

$$F_{z,LB} = a_6 \cdot \varepsilon_{yStr2} \tag{13}$$

a_i: Regression coefficient

170   Thereby the coefficients are derived from a calibration procedure using test bench measurements of statically applying single rotor load amplitudes to the DUT. This aims to reproduce calibration procedures of pulling a blade with a specific load, which is commonly done for validation of wind turbines (Lekou and Mouzakis, 2009). So in this study both commonly used approaches (analytic and calibrated) are considered to estimate main bearing loads from strain signals.

Additionally to these models, a third model using equations 10-13 is developed. Here, the regression coefficients are fitted to
175   complex load time series from training data (i.e., Table 1). This fitted model should therefore be a reference which accuracy can be achieved using strain signals under ideal conditions.

3.4 Displacement-based load estimation

Unlike a strain-based load estimation, there is no proven method for estimating main bearing loads from displacement signals. Using simplification to derive a linear equation system is not possible as main bearings do follow multidimensional nonlinear
180   stiffness curves. For this reason, an approach relying on regression models alone is used in this study. Using test bench measurements as training data different six different regression models are trained for main bearing load estimation.

A first model class for load estimation based on displacement signals is a simple linear regression (SLR) given by:

$$Y = \alpha_0 + \sum_{i=1}^{p} \alpha_i X_i \tag{14}$$

185   a_0/a_i: Regression coefficient

Y: Output Variable (Main bearing load)

X_i: Predictors (Displacement signals)

p: Number of predictors (Displacement signals)

190 Hereby, output variables are assumed to have a linear behavior to the predictors without any dependencies. To cover additional main effects, this linear model is expanded by the inclusion of predictor interactions. So a second model class is a linear regression with interactions (LRI) as follows:

$$Y = \alpha_0 + \sum_{i=1}^{p}\big(\alpha_i X_i + \sum_{j \in A_i}(\alpha_{ij} \cdot X_i \cdot X_j)\big), \qquad A_i = \{x \in [1, \dots, p] \mid x \neq i\} \tag{15}$$

195 a_{ij}:   Regression coefficient

This allows to determine the added value of taking into account the dependencies between the individual predictors. As a third model class the regression model is expanded by squared terms:

200 $$Y = \alpha_0 + \sum_{i=1}^{p}\big(\alpha_i X_i + \sum_{j=1}^{p}(\alpha_{ij} \cdot X_i \cdot X_j)\big), \tag{16}$$

Using linear regression with squared terms (LRS), output variables can show a nonlinear behavior to the individual predictors. This may be necessary due to progressive stiffness behavior of the main bearing itself.

Additionally to linear regression, random forest regression (RFR) is used to estimate main bearing loads from displacement
205 signals. Unlike curve based algorithms, the performance of RFR is almost not affected by nonlinear behavior of predictors and missing values or outliers within the training data can easily be handled. Another advantage of this algorithm is the comparatively good robustness against noise, which may be required due to a partially bad signal-to-noise-ratio of displacement signal.

Another algorithm used in this study is gaussian process regression (GPR). In addition to the achievable good accuracy of this
210 algorithm, there is the possibility to provide confidence intervals for the estimated loads. In this way, the uncertainty of estimated loads is considered in detail, what may be especially interesting in future evaluating a load history.

Finally, feedforward neural networks (FNN) are used for load estimation. Thereby FNN may give most flexible structure to model even strong nonlinear and unsteady relationships between loads and measurement signals. In previous simulation-based studies, this has been shown to achieve a significantly better accuracy compared to the benchmark of a SLR (Loriemi et al.,
215 2022).

### 3.5 Strain and displacement-based load estimation

Even though strain gauges may not be an option for long-term application today, recent developments show a further potential of this technology (Khosravani and Reinicke, 2020). The use of innovative 3D printing technologies makes it possible, in particular, to avoid sensitive bonding processes and to integrate the application into the component manufacturing process. So,

220 in addition to using strain or displacement signals separately, both types of signals combined are used to estimate main bearing loads. For this purpose, the same six regression algorithms are used that were previously introduced for displacement signals. Thus SLR, LRI, LRS, RFR, GPR and FNN models are developed using strain and displacement signals as predictors to evaluate the added value of the expansion by strain signals.

4. Results

225 Using the different regression models, the different main bearing loads of the testing data are estimated. Figure 5 shows an example of the difference between the actual applied load and the estimated loads of selected regression models. Models shown in this figure are both the analytically determined regression model and the calibrated regression model described in 2.2, an LRI using only displacement signals and an LRI using displacement and strain signals.
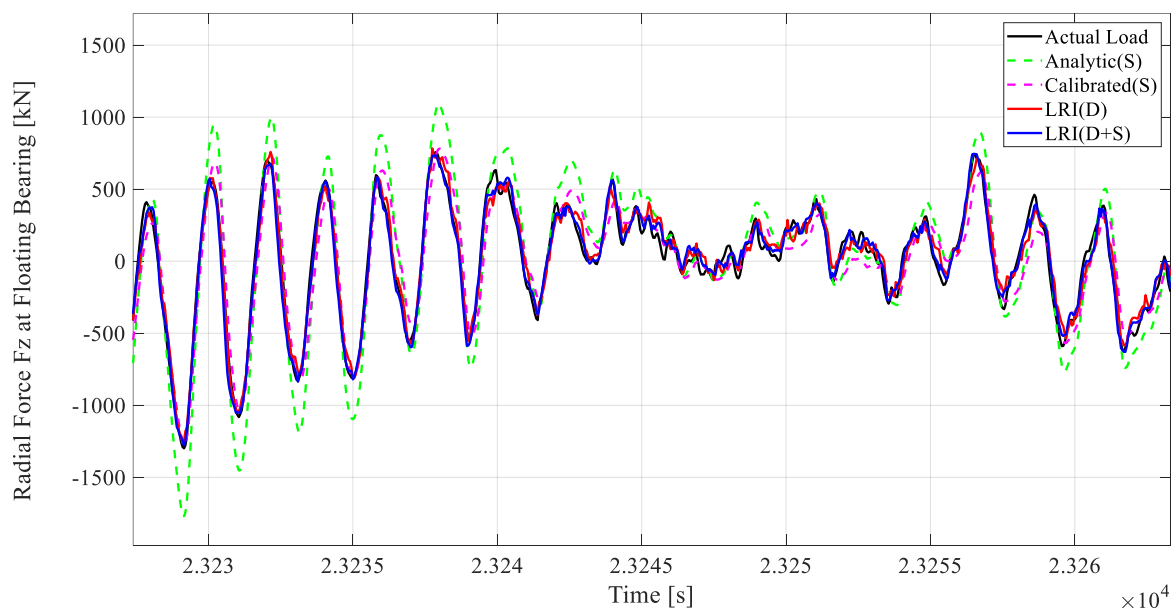
Figure 5. Actual and estimated floating bearing radial force in z-direction

In general, all models can reproduce the load profile, although qualitative differences can be found. The analytic determined regression model using strain signal as predictors, shows the largest deviation in the load estimate, whereas the calibrated model shows a significantly better performance. The smallest deviations are found for the two LRIs, whereby subjectively no

235 significant difference between the two models can be stated. In order to quantify the differences between the models, the following two performance parameters are evaluated. The root mean square error (RMSE) relatively to the covered load range and the coefficient of determination (R^2) defined in previous studies (Loriemi et al., 2022) are used to evaluate the performance

of the regression models. These results are shown in Table 2 and Table 3. Comparing performance parameters, it is clarified that the worst performing regression model is the analytically determined strain-based regression model. Especially for radial

240 loads of the floating bearing there is a more than doubled RMSE compared to most of the other regression models. This error is massively reduced by the calibration procedure of applying single loads to the DUT. The approach of using the training data (Table 1) to derive best fitting coefficients (cf. equation 10-13) results in the best performing regression model, which uses only strain signals and outperforms almost every displacement-based regression model. Regarding the displacement-based regression models, a performance equivalent to the strain-based models can be observed. Between the displacement-based

245 models, the SLR performs the worst. By including interactions into the regression model (cf. LRI) a significant improvement can be stated. Further increase of model complexity (i.e., LRS, GPR, RFR and ANN) does not significantly improve the estimation error. Regression models using both strain and displacement signals perform best, and comparison of these models among each other yields the same qualitative findings as those of the displacement-based models previously.

Table 2. RMSE of regression models

Regression Model	Signal type	RMSE/Load Range [%]				
		$Fy_{,FB}$	$Fz_{,FB}$	$Fx_{,LB}$	$Fy_{,LB}$	$Fz_{,LB}$
Analytic	S	5.5	5.4	~	2.3	2.1
Calibrated	S	2.8	2.9	~	2.0	2.1
Fitted	S	1.7	1.7	~	1.4	1.6
SLR	D	1.7	1.9	5.0	2.0	2.2
LRI	D	1.6	1.7	3.8	1.8	2.0
LRS	D	1.6	1.7	3.8	1.8	2.0
GPR	D	1.6	1.8	4.2	1.8	2.1
RFR	D	1.5	1.8	3.7	1.7	2.1
FNN	D	1.5	1.7	3.7	1.6	2.0
SLR	S+D	1.3	1.4	5.0	1.2	1.3
LRI	S+D	1.2	1.3	3.8	1.1	1.1
LRS	S+D	1.2	1.3	3.8	1.1	1.1
GPR	S+D	1.3	1.3	3.8	1.1	1.3
RFR	S+D	1.3	1.3	3.7	1.1	1.2
FNN	S+D	1.2	1.3	3.7	1.0	1.1
Load Range [MN]		4.4	4.5	0.68	4.5	4.4

S: Strain; D: Displacement; S+D: Strain and Displacement

250

Table 3. Coefficient of determination of regression models

Regression Model	Signal type	R^2 [%]				
		$Fy_{,FB}$	$Fz_{,FB}$	$Fx_{,LB}$	$Fy_{,LB}$	$Fz_{,LB}$
Analytic	S	55.4	66.2	~	92.2	95.5
Calibrated	S	88.9	91.2	~	94.5	95.6
Fitted	S	97.1	97.3	~	97.9	97.5
SLR	D	96.8	96.6	92.1	95.6	95.2
LRI	D	97.3	97.3	95.5	96.3	96.1
LRS	D	97.3	97.3	95.5	96.3	96.2
GPR	D	97.5	97.0	94.4	96.5	95.7
RFR	D	97.5	97.0	95.6	96.7	95.7
FNN	D	97.6	97.2	95.6	97.0	96.1
SLR	S+D	98.1	98.0	92.1	98.5	98.3
LRI	S+D	98.4	98.3	95.5	98.7	98.6
LRS	S+D	98.4	98.3	95.5	98.7	98.7
GPR	S+D	98.3	98.3	95.5	98.5	98.4
RFR	S+D	98.3	98.2	95.6	98.6	98.5
FNN	S+D	98.4	98.4	95.7	98.8	98.8

S: Strain; D: Displacement; S+D: Strain and Displacement

5. Discussion

From the results of this study, several findings regarding regression-based main bearing load estimation can be hold. One
255 finding was the strong deviation of the analytic and calibrated strain-based regression model. Comparing the analytically
calculated coefficients with the regression coefficients of the calibrated model, it can be stated that deviations mainly derive
from the young modulus. To achieve the same gain factors as the calibrated model, a 19 % higher young modulus for the AS
and a 11 % smaller young modulus of the MS would have been necessary. Gain factors have been calculated on basis of cross
section geometry and young modulus. Here, dimensions of the shafts have been measured on the test bench and young moduli
260 were given by the manufacturers of the AS and MS. As such strong deviations have not been measured for the geometry, it
has to be assumed that mainly fluctuations in the young modulus are the reason for this. In this context, fluctuations of up to
10.5 % have also been reported by Kock (Kock et al., 2018) and seem to be a general property of large-diameter shafts, which
is not represented by the young modulus uncertainty of 1.4 % assumed by Lekou (Lekou and Mouzakis, 2009). Based on these
results, the use of at least calibrated strain-based regression models is highly recommended, if main bearing load estimation is
265 performed using strain signals only.

The use of displacement signals for load estimation has been shown to provide an equivalent accuracy as using strain signals.
Because of the significant improvement of accuracy including interactions within regression (comparison of SLR and LRI) it
can be assumed that cross coupling effects contribute to the relationship between loads and displacements. On the other side

increasing model complexity does not improve accuracy as LRS, GPR, RFR and ANN have not shown better performance
than LRI. It can be assumed that the relationship between displacement signals and loads is not affected by strong
nonlinearities, the effect of which is significantly bigger than the present measurement errors.

Best regression results could be achieved using both displacement and strain signals combined. Especially regarding RMSE a
significant reduction compared to the regressions models only using displacement signals was possible. This suggests that both
types of signals can complement each other in this application. This may allow a reduced combined sensor setup without
significantly losing accuracy. A technically feasible variant in this application would be the use of axial displacement signals
on the rotor flange, which have good signal-to-noise-ratio due to the relatively large shaft deflection. These could then be
enhanced by well applicable strain gauges between the two main bearings measuring bending strains. This would avoid the
need for a large number of displacement sensors and reduce the cost of the measurement system. In addition, the strain
measurements before the first main bearing in this measurement setup (location x_{Str1} in Figure 1) would no longer be necessary.
Due to the usually inappropriate geometrical conditions between the rotor hub and the main bearing in real applications (i.e.,
short distance and noncylindrical shaft geometry), these would have been an unsuitable measuring location anyway.

Regardless of the signal types used, regression models with an R^2 of more than 95% could be developed which should already
be sufficient for evaluating fatigue-related damage or further investigations such as main bearing load loop identification (Hart,
2020). Comparing the load components, the estimation of the axial loads could only be performed with a significantly worse
performance than the estimation of radial loads. Here, the RMSE is more than doubled with respect to the covered load range.
This is also consistent with the results of simulative studies in which the same wind turbine was investigated (Loriemi et al.,
2022).

6. Conclusion

This paper has investigated the performance of regression models using strain and displacement signals for main bearing load
estimation. Neither strain nor displacement signals are identified as unsuitable or superior to each other. Comparing the
different regression models does not identify a superior method as most of the regression models have an equivalent
performance. Considering the use of only strain signals for load estimation, at least calibrated regression models are strongly
recommended, otherwise poor performance of an analytically determined model is risked due to the large variations of the
young modulus. All regression models have shown adequate accuracy. Therefore, future work should mainly focus on two
aspects. First, since very good accuracies are already achieved with almost all methods, the costs of the measurement system
can be reduced (e.g., usage of less sensors) without significantly losing accuracy. Second, as test bench measurements were
used as training data in this paper, it should be analyzed if this expensive data base could be substituted with other data sources.
Previous studies (Loriemi et al., 2022) have proposed to use simulation data for this purpose. Therefore, it remains to be
clarified whether sufficient quality of simulation results can be achieved so that a still good load estimation accuracy can be
obtained.

References

Becker, M.: The Maxcap Wind Turbine - A comprehensive approach for an optimised drive train and power conversion system, Conference
for Wind Power Drives 2019, Aachen, 259-275, 2019.

310 Berg, J. C., Resor, B. R., Paquette, J. A., and White, J. R.: SMART wind turbine rotor: design and field test, SAND2014-0681, Sandia
National Laboratories, Albuquerque, NM, 2014.

Bezziccheri, M., Castellini, P., Evangelisti, P., Santolini, C., and Paone, N.: Measurement of mechanical loads in large wind turbines:
Problems on calibration of strain gage bridges and analysis of uncertainty, Wind Energy, 20, 1997-2010, 2017.

Enevoldsen, P. and Xydis, G.: Examining the trends of 35 years growth of key wind turbine components, Energy for sustainable development,
315 50, 18-26, 2019.

Gnauert, J., Jacobs, G., Kock, S., Bosse, D., and Janik, B.: Design study for a multicomponent transducer for wind turbine test benches,
Journal of Sensors and Sensor Systems, 9, 239-249, 2020.

Guy, B.: Measurement and traceability of torque on large mechanical drives, Sensor 2015, Nuremberg, 44 - 45, 10.5162/sensor2015/A1.3,

Hart, E.: Developing a systematic approach to the analysis of time-varying main bearing loads for wind turbines, Wind Energy, 23, 2150-
320 2165, 2020.

Hart, E., Turnbull, A., Feuchtwang, J., McMillan, D., Golysheva, E., and Elliott, R.: Wind turbine main-bearing loading and wind field
characteristics, Wind Energy, 22, 1534-1547, 2019.

Hart, E., Clarke, B., Nicholas, G., Kazemi Amiri, A., Stirling, J., Carroll, J., Dwyer-Joyce, R., McDonald, A., and Long, H.: A review of
wind turbine main bearings: design, operation, modelling, damage mechanisms and fault detection, Wind Energy Science, 5, 105-124, 2020.

325 Helsen, J., Peeters, P., Vanslambrouck, K., Vanhollebeke, F., and Desmet, W.: The dynamic behavior induced by different wind turbine
gearbox suspension methods assessed by means of the flexible multibody technique, Renewable Energy, 69, 336-346, 2014.

Khosravani, M. R. and Reinicke, T.: 3D-printed sensors: Current progress and future challenges, Sensors and Actuators A: Physical, 305,
111916, https://doi.org/10.1016/j.sna.2020.111916, 2020.

Kock, S., Jacobs, G., Bosse, D., and Strangfeld, F.: Simulation Method for the Characterisation of the Torque Transducers in MN· m range,
330 Journal of Physics: Conference Series, 042014,

Lekou, D. and Mouzakis, F.: WT load measurement uncertainty: load-based versus analytical strain-gauge calibration method, Journal of
solar energy engineering, 131, 2009.

Loriemi, A., Jacobs, G., and Bosse, D.: Estimation of rotor and main bearing loads using artificial neural networks, Journal of Physics:
Conference Series, 012002,

335 Noppe, N., Weijtjens, W., and Devriendt, C.: Modeling of quasi-static thrust load of wind turbines based on 1 s SCADA data, Wind Energy
Science, 3, 139-147, 2018.

Pagitsch, M., Jacobs, G., and Bosse, D.: Remaining Useful Life Determination for Wind Turbines, Journal of Physics: Conference Series,
012052,

Pierce, K. G. and Lemieux, D. L.: Method and apparatus for wind turbine rotor load control, 2007.

340 Pierce, K. G., Lemieux, D. L., and Blakemore, R. W.: Method and apparatus for wind turbine rotor load control based on shaft radial
displacement, 2006.

Reisch, S., Jacobs, G., Bosse, D., and Matzke, D.: Challenges and opportunities of full size nacelle testing of wind turbine generators, The
Proceedings of the JSME international conference on motion and power transmissions 2017, Kyoto, 10-01,

Verbruggen, T., Rademakers, L., and Braam, H.: Fibre Optic Blade Monitoring for optimisation of offshore wind farm O&M, ECN-E–012-
345   018, 2012.

Yucesan, Y. A. and Viana, F.: Onshore wind turbine main bearing reliability and its implications in fleet management, AIAA Scitech 2019
Forum, 1225,